Polyhedron 90 (2015) 47–57

Contents lists available at ScienceDirect

Polyhedron

journal homepage: www.elsevier.com/locate/poly

Coordination polymers and molecular structures among complexes of mercury(II) halides with selected 1-benzoylthioureas

Andrzej Okuniewski *, Damian Rosiak, Jarosław Chojnacki, Barbara Becker

Department of Inorganic Chemistry, Chemical Faculty, Gdańsk University of Technology, G. Narutowicza 11/12, 80-233 Gdańsk, Poland

ARTICLE INFO

Article history:
Received 7 November 2014
Accepted 31 January 2015
Available online 9 February 2015

Keywords:
Mercury complexes
Coordination polymers
Benzoylthioureas
Coordination center geometry
Rod group symmetry

ABSTRACT

Six new 1-benzoyl-3-phenylthiourea and 1-benzoyl-3-(2-methylphenyl)thiourea complexes of mercury(II) were obtained in the reactions of the ligands with HgX_2 in methanol (X = Cl, Br, I). Their structures, determined by single-crystal X-ray diffraction analysis, exhibit different stoichiometries and molecular organization. Coordination centers adopt more or less distorted tetrahedral geometry (five structures) or distorted trigonal bipyramidal geometry (one structure). In four cases 1D coordination polymers were formed and in the other two molecular compounds were found. In three cases solvent molecules (H_2O or MeOH) were found in crystal structure. Although all compounds share common intramolecular N–H···O=C structural motif they exhibit unique hydrogen bonding pattern. Common $\mathscr{P}c11$ rod group symmetry of polymer chains (where applicable) allows simplified classification of the 3D packing as parallel stacking of trapezoidal prisms.

1. Introduction

Thiourea and its derivatives found many applications in analytical chemistry [1], heterocyclic synthesis [2], metal flotation, leaching and extraction [3,4], rubber processing [5,6] and many others [7]. Especially interesting group of thiourea derivatives are acylthioureas [8] due to the simple synthesis [9], their stability and biological activity [10,11].

According to Pearson's HSAB theory [12], the mercury(II) ions are soft Lewis acids and thiourea derivatives are soft Lewis bases, so they are likely to form strong coordination bonds. Therefore, extensive studies are conducted to examine chemistry of these species. It is very important, because mercury compounds exhibit high toxicity to living organisms and their chelation can help in human detoxification [13]. Other *S*-donor ligands commonly used for mercury(II) complexation are: dithiocarbamates [14,15], thiosemicarbazones [16] and thiocyanates [17].

During our research we have synthesized new complexes of 1-benzoyl-3-phenylthiourea (bptu) and 1-benzoyl-3-(2-methylphenyl)thiourea (bmtu) with mercury(II) halides:

$$n\mathrm{HgX_2} + n\mathrm{xL} \xrightarrow{\mathrm{MeOH}} [\mathrm{HgX_2L}_x]_n \cdot n\mathrm{So}$$

	L	X	*N*	*x*	So
1	bptu	Cl	1	2	MeOH
2	bptu	Br	∞	1	H_2O
3	bptu	I	∞	1	—
4	bmtu	Cl	∞	1	H_2O
5	bmtu	Br	∞	1	—
6	bmtu	I	1	2	—

We have obtained and structurally characterized six new compounds: bis(1-benzoyl-3-phenylthiourea-κ*S*)dichloromercury(II) methanol monosolvate (**1**), *catena*-poly[[(1-benzoyl-3-phenylthiourea-κ*S*)mercury(II)]-di-μ-bromo monohydrate] (**2**), *catena*-poly[[(1-benzoyl-3-phenylthiourea-κ*S*)iodomercury(II)]-μ-iodo] (**3**), *catena*-poly[[(1-benzoyl-3-(2-methylphenyl)thiourea-κ*S*)chloromercury(II)]-μ-chloro monohydrate] (**4**), *catena*-poly[[(1-benzoyl-3-(2-methylphenyl)thiourea-κ*S*)bromomercury(II)]-μ-bromo] (**5**) and bis(1-benzoyl-3-(2-methylphenyl)thiourea-κ*S*)diiodomercury(II) (**6**). Four of them are coordination polymers [18–20] – for nomenclature, see: [21].

2. Experimental

2.1. Synthesis of ligands

Thiourea derivatives were prepared according to procedure proposed by Douglas and Dains [9]: 92 mmol of ammonium

* Corresponding author. Tel.: +48 58 347 2522.
E-mail address: andrzej.okuniewski@gmail.com (A. Okuniewski).

http://dx.doi.org/10.1016/j.poly.2015.01.035
0277-5387/

thiocyanate and 60 ml of acetone were placed in a two-necked flask. Through the dropping funnel 80 mmol of benzoyl chloride in 20 ml of acetone was added with stirring. After addition was complete the mixture was refluxed for additional 15 min and then 80 mmol of amine in 30 ml of acetone was added through the dropping funnel. Reaction mixture was poured into 500 ml of water with stirring. The resulting precipitate was filtered on a Büchner funnel. Crude product was recrystallized from acetone.

1-Benzoyl-3-phenylthiourea (bptu) [22] was obtained with 87% yield. Mp.: 160(1) °C. ^{1}H NMR: δ (500 MHz, $CDCl_3$, ppm) = 7.26–7.91 (*m*, 10H), 9.12 (*s*, 1H), 12.60 (*s*, 1H).

1-Benzoyl-3-(2-methylphenyl)thiourea (bmtu) [23] was obtained with 89% yield. Mp.: 117(1) °C. ^{1}H NMR: δ (500 MHz, $CDCl_3$, ppm) = 2.38 (*s*, 3H), 7.24–7.93 (*m*, 9H), 9.21 (*s*, 1H), 12.27 (*s*, 1H).

Full ^{1}H NMR spectra for bptu and bmtu are provided in Supplementary materials (Figs. s1 and s2).

2.2. Synthesis of complexes

All complexes were synthesized by the general procedure as follows: 1 mmol of commercially available HgX_2 (X = Cl, Br, I) and 1 mmol of thiourea derivative (see above) were added to 35 ml of methanol, the mixture was stirred for 15 min and then filtrated. The filtrate was left to slowly evaporate at room temperature.

For **1**, 0.27 g of $HgCl_2$ and 0.26 g of bptu were used. After several days colorless plates were isolated with 42% yield. Mp.: 118(1) °C. Elem. Anal. Calc. for $C_{29}H_{28}Cl_2HgN_4O_3S_2$: C, 42.68; H, 3.46; N, 6.86; S, 7.86. Found: C, 42.70; H, 3.45; N, 7.03; S, 7.85%.

For **2**, 0.36 of $HgBr_2$ and 0.26 g of bptu were used. After several days colorless plates were isolated with 15% yield. Mp.: 152(1) °C – dehydration, 168(1) °C – melting point. Elem. Anal. Calc. for $C_{14}H_{14}Br_2HgN_2O_2S$: C, 26.49; H, 2.22; N, 4.41; S, 5.05. Found: C, 26.04; H, 2.17; N, 4.36; S, 5.22%.

For **3**, 0.45 g of HgI_2 and 0.26 g of bptu were used. After several days pale yellow plates were isolated with 33% yield. Mp.: 147(1) °C. Elem. Anal. Calc. for $C_{14}H_{12}HgI_2N_2OS$: C, 23.66; H, 1.70; N, 3.94; S, 4.51. Found: C, 23.58; H, 1.72; N, 3.98; S, 4.57%.

For **4**, 0.27 g of $HgCl_2$ and 0.27 g of bmtu were used. After several days colorless plates were isolated with 70% yield. Mp.: 168(1) °C. Elem. Anal. Calc. for $C_{15}H_{16}Cl_2HgN_2O_2S$: C, 32.18; H, 2.88; N, 5.00; S, 5.73. Found: C, 32.19; H, 2.87; N, 5.02; S, 5.88%.

For **5**, 0.36 g of $HgBr_2$ and 0.27 g of bmtu were used. After one day colorless blocks were isolated with 59% yield. Mp.: 184(1) °C. Elem. Anal. Calc. for $C_{15}H_{14}Br_2HgN_2OS$: C, 28.56; H, 2.24; N, 4.44; S, 5.08. Found: C, 28.31; H, 2.21; N, 4.40; S, 5.13%.

For **6**, 0.45 g of HgI_2 and 0.27 g of bmtu were used. After several minutes colorless plates were isolated with 35% yield. Mp.: 188(1) °C. Elem. Anal. Calc. for $C_{30}H_{28}HgI_2N_4O_2S_2$: C, 36.21; H, 2.84; N, 5.63; S, 6.44. Found: C, 35.92; H, 2.86; N, 5.69; S, 6.54%.

Far Infra-Red spectra (600–50 cm^{-1}) for **1**–**6** are provided in supplementary materials (Fig. s3).

2.3. Measurements

X-ray diffraction measurements were carried out with a KM4 diffractometer (Kuma Diffraction, Wroclaw, Poland) with CCD detector (Oxford Diffraction, Yarnton, United Kingdom) using graphite monochromated Mo Kα radiation at 298 K. The structures were solved by direct methods and refined anisotropically using the program packages WinGX 2013.3 [24] and SHELX-2013 [25]. Positions of the hydrogen atoms were calculated geometrically (except of those in OH groups) and taken into account with isotropic temperature factors. Further information on crystal structure refinement can be found in Table 1.

Elemental analyses were carried on Vario El Cube (Elementar Analysensysteme GmbH, Hanau, Germany).

^{1}H NMR spectra were collected on Unity 500 plus (Varian, California, United States) spectrometer in chloroform-d at room temperature.

Far Infra-Red spectra were collected on Nicolet 8700 (Thermo Electron, Massachusetts, United States) spectrometer with polyethylene windows in Nujol at room temperature.

Melting points were measured on SMP30 (Stuart, Stone, United Kingdom) and were uncorrected.

2.4. Auxiliary structural parameters

In analysis of coordination polyhedra in presented structures we have used three structural index parameters. For five-coordinate complexes the τ_5 is in common use [26]. If $\beta > \alpha$ are the two greatest valence angles, then its value indicates whether the structure is square pyramidal ($\tau_5 = 0$), trigonal bipyramidal ($\tau_5 = 1$), or somewhere in between:

Table 1
Crystal and final structure refinement data for $[HgCl_2(bptu)_2]\cdot MeOH$ (**1**), $[HgBr_2(bptu)]_n\cdot nH_2O$ (**2**), $[HgI_2(bptu)]_n$ (**3**), $[HgCl_2(bmtu)]_n\cdot nH_2O$ (**4**), $[HgBr_2(bmtu)]_n$ (**5**) and $[HgI_2(bmtu)_2]$ (**6**).

Compound reference	**1** (CCDC 971976)	**2** (CCDC 971977)	**3** (CCDC 971978)	**4** (CCDC 971979)	**5** (CCDC 971980)	**6** (CCDC 971981)
Chemical formula	$C_{29}H_{28}Cl_2HgN_4O_3S_2$	$C_{14}H_{14}Br_2HgN_2O_2S$	$C_{14}H_{12}HgI_2N_2OS$	$C_{15}H_{16}Cl_2HgN_2O_2S$	$C_{15}H_{14}Br_2HgN_2OS$	$C_{30}H_{28}HgI_2N_4O_2S_2$
M (g/mol)	816.16	634.74	710.71	559.85	630.75	995.07
Crystal system	orthorhombic	orthorhombic	orthorhombic	orthorhombic	monoclinic	monoclinic
Space group	*Pbca*	*Pbca*	*Pbca*	*Pbca*	$P2_1/c$	$C2/c$
a (Å)	17.9343(11)	18.5937(14)	10.8279(5)	19.4695(12)	11.8229(7)	20.921(2)
b (Å)	11.9226(6)	7.5632(4)	8.7422(5)	7.5529(5)	20.5663(9)	8.7913(6)
c (Å)	29.1985(12)	24.6859(18)	37.5981(19)	23.982(4)	7.8419(4)	20.216(3)
β (°)	90	90	90	90	103.466(6)	118.344(14)
V (Å^3)	6243.3(6)	3471.5(4)	3559.0(3)	3526.5(6)	1854.36(17)	3272.3(7)
Z	8	8	8	8	4	4
F(000)	3200	2352	2560	2128	1168	1880
D_{calc}, (g/cm^3)	1.737	2.429	2.653	2.109	2.259	2.020
μ, (1/mm)	5.27	13.60	12.24	9.16	12.72	6.75
N_{ref}	14388	21104	21074	22149	6849	5714
N_{ref} [independent]	6130	3410	3495	3464	3651	3194
N_{ref} [$I > 2\sigma(I)$]	4174	2152	2873	2374	2403	2394
R_{int}	0.052	0.114	0.066	0.113	0.035	0.042
R	0.059	0.077	0.059	0.071	0.046	0.051
wR	0.147	0.234	0.153	0.194	0.121	0.135

$$\tau_5 = \frac{\beta - \alpha}{60^\circ}$$

For four-coordinate structures the τ_4 parameter was developed [27]. If the structure is square planar, then $\tau_4 = 0$, while for tetrahedral structures $\tau_4 = 1$ (α and β like before; $\theta = \cos^{-1}(-1/3) \approx 109.5^\circ$ is tetrahedral angle):

$$\tau_4 = \frac{360^\circ - (\alpha + \beta)}{360^\circ - 2\theta}$$

Unfortunately the above formula does not distinguish α and β angles, so structures of significantly different geometries can have similar τ_4 value. To overcome this issue we propose another structural index parameter τ'_4 that adopts values similar to τ_4, however better differentiates the examined structures ($\tau'_4 \lesssim \tau_4$):

$$\tau'_4 = \frac{\beta - \alpha}{360^\circ - \theta} + \frac{180^\circ - \beta}{180^\circ - \theta}$$

To describe degree of aromaticity of some rings we have used HOMA (Harmonic Oscillator Model of Aromaticity) index defined as [28]:

$$\mathrm{HOMA} = 1 - \frac{1}{N}\sum_{n=1}^{N}\alpha_n(R_n - \bar{R}_n)^2$$

where N is the number of bonds, R_n is the individual bond length, $\bar{R}_n$ is the optimal value of n-th bond length in aromatic compound, α_n is a normalization constant. For CN bond $\bar{R} = 1.334$, $\alpha = 93.52$; for CO bond $\bar{R} = 1.265$, $\alpha = 157.38$. For fully aromatic compounds HOMA is equal to 1, while for non-aromatic compounds it is equal to 0.

In description of parallel-displaced stacking interactions the following parameters are given: d – centroid–centroid distance, α – dihedral angle between ring planes, *slippage* – distance between the first centroid and perpendicular projection of the second centroid on the plane of the first ring and *vice versa* (only when $\alpha = 0$). For more information on stacking interactions in mercury(II) complexes, see: [29–31].

Isostructural systems were analyzed using two parameters. The first was unit cell identity parameter Π [32] which is defined by the following formula (for identical unit cells $\Pi = 0$):

$$\Pi_{i,j} = \frac{a_i + b_i + c_i}{a_j + b_j + c_j} - 1$$

where $a_i + b_i + c_i > a_j + b_j + c_j$ are orthogonalized unit cell parameters of the crystals i and j. The second was isostructurality index I' [33] (for two identical structures $I' = 1$):

$$I'_{i,j} = 1 - \sqrt{\frac{q}{N}\sum_{n=1}^{N}[(x_{i,n} - x_{j,n})^2 + (y_{i,n} - y_{j,n})^2 + (z_{i,n} - z_{j,n})^2]}$$

where $x_{i,n}$, $x_{j,n}$, $y_{i,n}$, $y_{j,n}$, $z_{i,n}$ and $z_{j,n}$ are crystallographic coordinates of corresponding n-th non-hydrogen atom in structure i and j, N is the total number of atoms in one structure and q depends on size of asymmetric unit.

For description of graph-set notation of hydrogen bond motifs, see: [34].

In the following discussion $Cg(n)$ symbol will designate C(10n + 1)–C(10n + 6) aromatic ring and $CgS(n)$ will designate pseudoaromatic ring that incorporates N(n + 1)–H···O(n) hydrogen bond.

3. Results

3.1. Crystal structure of **1**

Crystals of **1** are composed of mononuclear complex molecules, where four-coordinated mercury ($HgCl_2S_2$ coordination sphere) adopts slightly distorted tetrahedral geometry with $\tau_4 = \tau'_4 = 0.92$ (Fig. 1). The whole molecule is asymmetric. Hg–S and Hg–Cl bond lengths are typical, the angles on S atoms are 108.9(3)° and 105.6(3)° indicating high contribution of pure p-orbital in the bond.

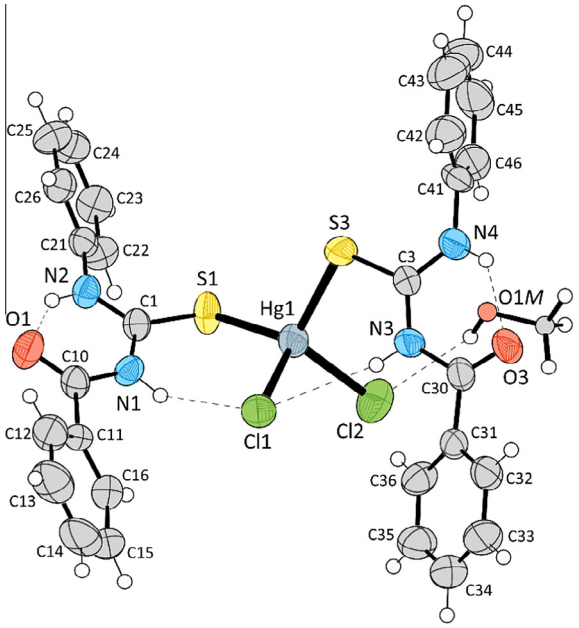

Fig. 1. Molecular structure of **1**. Ellipsoids are drawn at 50% probability level (except solvent molecule). Selected hydrogen bonds are denoted with dashed lines. Key bond lengths (Å) and angles (°) are: Hg1–S1 2.488(3), Hg1–S3 2.514(3), Hg1–Cl1 2.528(3), Hg1–Cl2 2.473(3), S1–Hg1–S3 115.98(9), S1–Hg1–Cl1 113.81(8), S1–Hg1–Cl2 108.85(10), S3–Hg1–Cl1 100.79(9), S3–Hg1–Cl2 111.47(11), Cl1–Hg1–Cl2 105.31(10).

Within the complex molecule N1–H···Cl1 and N3–H···Cl1 hydrogen bonds are present. Solvating methanol is connected to complex *via* O1*M*–H···Cl2 hydrogen bond. Ligand molecules adopt classic S-type conformation [35] with intramolecular N2–H···O1 and N4–H···O3 hydrogen bonds forming **S**(6) motifs. The latter bond is bifurcated and contributes in a formation of centrosymmetric dimers *via* N4–H···O3$^{[1-x,\ 1-y,\ -z]}$ hydrogen bonds. In this way a centrosymmetric $\mathbf{R}_2^2(12)$ ring is formed. All hydrogen bonds are visualized in Fig. 2 and their parameters are summarized in Table 2.

The strongest parallel-displaced stacking interaction is quite weak: $Cg2\cdots Cg3^{[1-x,\ -½+y,\ ½-z]}$ with $d = 4.16$ Å and $\alpha = 10°$. Twist of aromatic rings in the relation to **S**(6) planes (see: Table s4) can

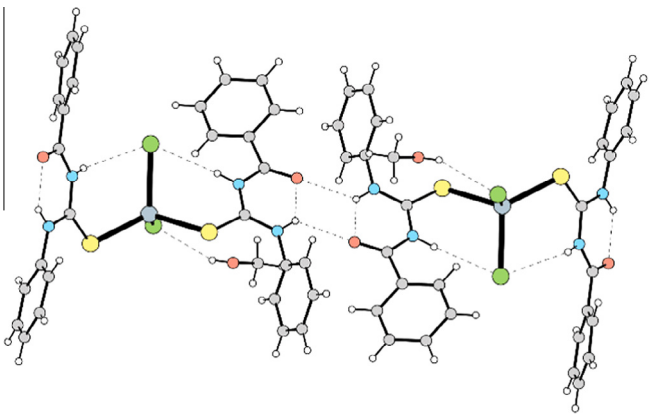

Fig. 2. Centrosymmetric dimer and hydrogen bond pattern found in structure of **1**. Hydrogen bonds are denoted with dashed lines.

Table 2
Hydrogen bond parameters in structure of **1**. Symmetry operation: (a) $1-x, 1-y, -z$.

	D–H (Å)	H···A (Å)	D···A (Å)	D–H···A (°)
N2–H2···O1	0.86	1.92	2.616(11)	136
N1–H1···Cl1	0.86	2.68	3.385(9)	141
N3–H3···Cl1	0.86	2.70	3.548(9)	168
N4–H4···O3	0.86	1.98	2.645(10)	133
N4–H4···O3[a]	0.86	2.50	3.177(12)	137
O1*M*–H1*M*···Cl2	0.82	2.45	3.14(2)	142

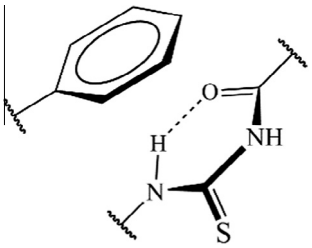

Fig. 3. Schematic visualization of Ph···**S**(6) interaction.

be rationalized by the formation of non-parallel stacking interactions. E.g. C32–H and C33–H donors interact with $Cg4^{[1-x,\ 1-y,\ -z]}$ ring (d = 4.52 Å, α = 50°) as well as C15–H and C16–H interact with $Cg2^{[½+x,\ y,\ ½-z]}$ ring (d = 4.31 Å, α = 65°) to form edge-to-face stacking. Additionally the C42–H···$Cg1^{[1-x,\ ½+y,\ ½-z]}$ T-shaped interaction can be found (d = 5.26 Å, α = 64°).

As the mobility of electrons within the **S**(6) motif is significant, the fragment can be considered as the aromatic ring (Fig. 3). HOMA values for *Cg*S1 and *Cg*S3 rings are 0.81 and 0.80, respectively. Furthermore, as the polarity of such a hydrogen bond motif is higher, the range of inter-ring distances for effective interaction may be wider as compared to pure hydrocarbon aromatic rings. Nevertheless, their contribution to overall stabilization energy should not be overestimated.

We note the presence of the $Cg1\cdots CgS3^{[1-x,\ -½+y,\ ½-z]}$ interaction. Parameters of this interaction are: d = 4.55 Å, α = 18°. Similar interactions can be found in various structures deposited in the CSD, e.g. in salicylideneaniline derivatives [36].

All the interactions lead to the formation of 3D structure of **1** (Fig. 4).

3.2. Crystal structure of *2*

Compound **2** exhibits five-coordinate structure ($HgBr_4S$ coordination sphere) with four bridging bromide ions around the mercury(II) (Fig. 5). Until now, only 7 solved structures of complexes with HgX_4S coordination sphere were deposited in the CSD. Bridging Hg–Br bonds are unsymmetrical: two of them are longer by ca. 0.5 Å, so one can even regard them as short contacts (see: Table s4). In the case of **2** structural index parameter equals to τ_5 = 0.72, indicating that the geometry of coordination kernel is closer to trigonal

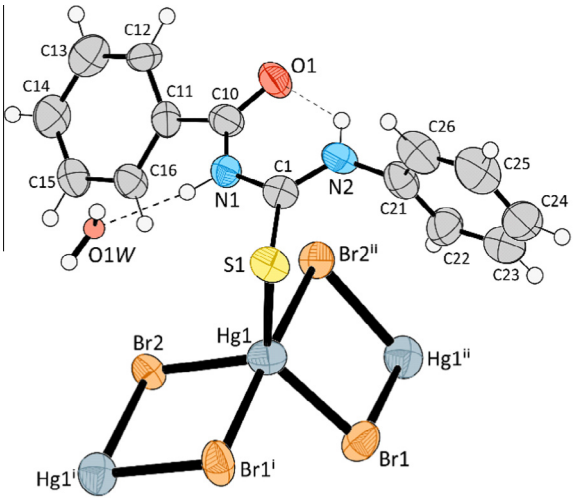

Fig. 5. Molecular structure of **2**. Ellipsoids are drawn at 50% probability level (except the solvent molecule). Selected hydrogen bonds are denoted with dashed lines. Key bond lengths (Å) and angles (°) are: Hg1–S1 2.461(4), Hg1–Br1 2.5273(18), Hg1–Br2 2.6054(17), Hg1–Br1^{i} 3.0329(17), Hg1–Br2^{ii} 3.1881(17), S1–Hg1–Br1 129.91(11), S1–Hg1–Br2 115.45(10), S1–Hg1–Br1^{i} 91.47(10), S1–Hg1–Br2^{ii} 95.42(10), Br1–Hg1–Br2 114.64(6), Br1–Hg1–Br1^{i} 88.80(5), Br1–Hg1–Br2^{ii} 87.00(5), Br2–Hg1–Br1^{i} 88.98(5), Br2–Hg1–Br2^{ii} 87.81(5), Br1^{i}–Hg1–Br2^{ii} 173.10(5). Symmetry operations: (i) ½ − *x*, −½ + *y*, *z*; (ii) ½ − *x*, ½ + *y*, *z*.

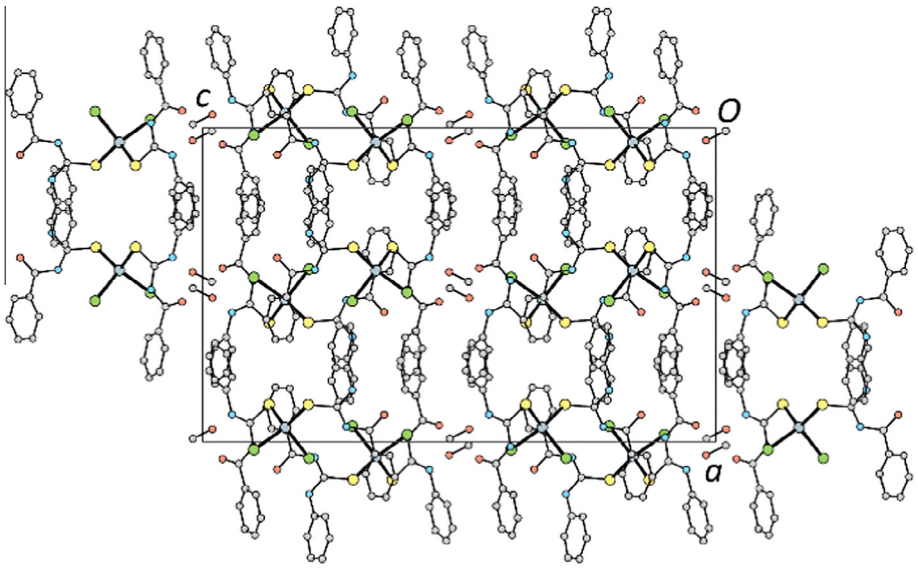

Fig. 4. Crystal packing in **1** seen along [0 1 0] direction. Hydrogen atoms are omitted for clarity.

bipyramidal than to square pyramidal. Bridging by bromide ions lead to the formation of coordination polymer with chain spreading along [0 1 0] direction and with identity period equal to the unit cell *b* parameter. Each chain has $\not{p}c11$ (R5) rod group symmetry [37] and trapezoidal prism shape with the glide plane passing through centers of the parallel sides of trapezoid (Fig. 6). Packing of those parallel rods form the final 3D crystal structure.

Like in **1**, the ligand molecule adopts S-type conformation with intramolecular N2–H···O1 hydrogen bond forming **S**(6) motif (Fig. 5). It is also bifurcated and couples chains *via* intermolecular N2–H···O1$^{[-x,\ 2-y,\ -z]}$ hydrogen bond (Fig. 7). Solvating water molecule stabilizes the structure by fastening different chains of coordination polymer *via*: N1–H···O1*W*, O1*W*–H···O1$^{[-x,\ 1-y,\ -z]}$ and O1*W*–H···Br2$^{[½-x,\ -½+y,\ z]}$ hydrogen bonds. All hydrogen bonds parameters are summarized in Table 3.

We note the absence of parallel-displaced stacking interactions between phenyl rings, however three T-shaped stacking interactions can be found. Two of them form *Cg*2$^{[-x,\ 2-y,\ -z]}$···H–C12[*Cg*1]C15–H···*Cg*1$^{[½-x,\ -½+y,\ z]}$ motif (parameters are: d = 4.72 Å, α = 58° and d = 4.96 Å, α = 60°, respectively). Additionally there is C26–H···*Cg*1$^{[-x,\ 1-y,\ -z]}$ interaction (d = 4.94 Å, α = 58°). Also C23–H and C24–H donors interact with *Cg*2$^{[-x,\ ½+y,\ ½-z]}$ to form edge-to-face stacking (d = 5.26 Å, α = 64°). These interactions rationalize twist of aromatic rings in the relation to **S**(6) planes (see: Table s4).

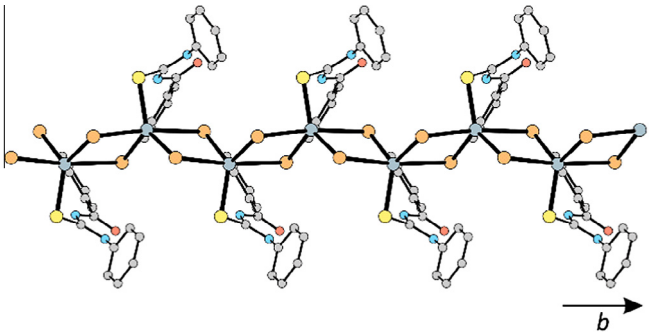

Fig. 6. Coordination polymer chain with $\not{p}c11$ rod symmetry in structure of **2**. Hydrogen atoms and solvent molecules are omitted for clarity.

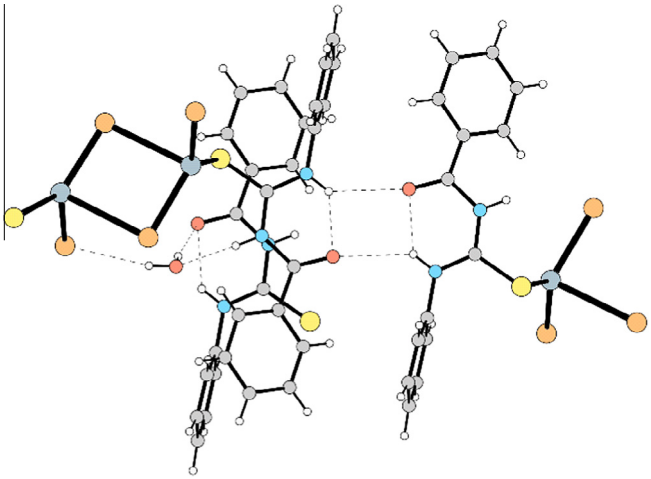

Fig. 7. Centrosymmetric dimer and hydrogen bond pattern found in structure of **2**. Hydrogen bonds are denoted with dashed lines.

Table 3
Hydrogen bond parameters in structure of **2**. Symmetry operations: (a) $-x$, $2-y$, $-z$; (b) $-x$, $1-y$, $-z$; (c) $½-x$, $-½+y$, z.

	D–H (Å)	H···A (Å)	D···A (Å)	D–H···A (°)
N2–H2···O1	0.86	2.01	2.659(16)	131
N2–H2···O1^{a}	0.86	2.46	3.169(15)	140
N1–H1···O1*W*	0.86	2.04	2.881(17)	167
O1*W*–H1*W*···O1^{b}	0.83	2.41	3.230(16)	170
O1*W*–H2*W*···Br2^{c}	0.83	2.63	3.444(14)	168

An interaction of two pseudo-aromatic **S**(6) motifs from two different polymer chains is also present: *Cg*S1···*Cg*S1$^{[-x,\ 1-y,\ -z]}$ (*Cg*S1 HOMA = 0.84). Parameters are: d = 4.25 Å, α = 0°, *slippage* = 2.26 Å.

Packing of molecules in unit cell is presented in Fig. 8.

3.3. Crystal structure of **3**

Mercury(II) in solvent-free compound **3** is connected to three iodide anions and one bptu molecule forming HgI_3S kernel with highly distorted tetrahedral geometry, τ_4 = 0.71, τ'_4 = 0.67 (Fig. 9). Unlike I2, the I1 ion is a bridging ligand that allows the formation of coordination polymer. Similarly as in **2**, chains spread along [0 1 0] direction and have $\not{p}c11$ rod group symmetry (Fig. 10). Ligand molecules also adopt the same S-type conformation with **S**(6) hydrogen bond motif *via* N2–H···O1. Additionally there is an intramolecular hydrogen bond: N1–H1···I2. Parameters for both hydrogen bonds are summarized in Table 4.

The strongest parallel-displaced stacking interaction in this structure is *Cg*1···*Cg*1$^{[1-x,\ 2-y,\ -z]}$ with d = 4.43 Å, α = 0°, *slippage* = 2.77 Å, which could be neglected. Additionally there is *Cg*1···*Cg*S1$^{[3/2-x,\ ½+y,\ z]}$ interaction with d = 3.84 Å, α = 5° (*Cg*S1 HOMA = 0.75). Twist of phenyl ring on N2 in the relation to **S**(6) motif in **3** is lowest among described structures (see: Table s4). This is probably because of lack of non-parallel stacking interactions.

The packing of parallel-aligned polymer chains is presented in Fig. 11.

3.4. Crystal structure of **4**

In structure of **4** three chloride anions and one bmtu molecule are bonded to mercury(II) forming $HgCl_3S$ kernel that exhibit highly distorted tetrahedral geometry with τ_4 = 0.82, τ'_4 = 0.76 (Fig. 12). Similarly to **3**, the halogen (Cl1) atom serves as a bridging ligand and coordination polymer with chain of $\not{p}c11$ rod group symmetry spreading in [0 1 0] direction is formed (Fig. 13). Again the chains are parallel-aligned.

Ligand molecule adopts S-type conformation with **S**(6) hydrogen bond motif. Like in **2**, such hydrogen bond is bifurcated and centrosymmetric dimer is formed: N2–H···O1 and N2–H···O1$^{[-x,\ 2-y,\ -z]}$ (Fig. 14). Water molecule present in this structure is relatively weakly bonded *via* N1–H···O1*W* and O1*W*–H···Cl2 hydrogen bonds. Relevant parameters are summarized in Table 5.

No simple parallel-displaced stacking interactions can be found in this structure, but an interesting feature is the stacking of two pseudo-aromatic **S**(6) motifs: *Cg*S1···*Cg*S1$^{[-x,\ 1-y,\ -z]}$ with d = 4.51 Å, α = 0°, *slippage* = 1.97 Å (*Cg*S1 HOMA = 0.82). Twist of *o*-tolyl group is large in this case (see: Table s4), what is probably caused by formation of edge-to-face interactions between C12–H and C13–H donors with *Cg*2$^{[-x,\ 2-y,\ -z]}$ ring (d = 4.56 Å, α = 57°). These interactions give additional stabilization energy to the centrosymmetric dimer formation.

Packing of polymer chains is presented in Fig. 15.

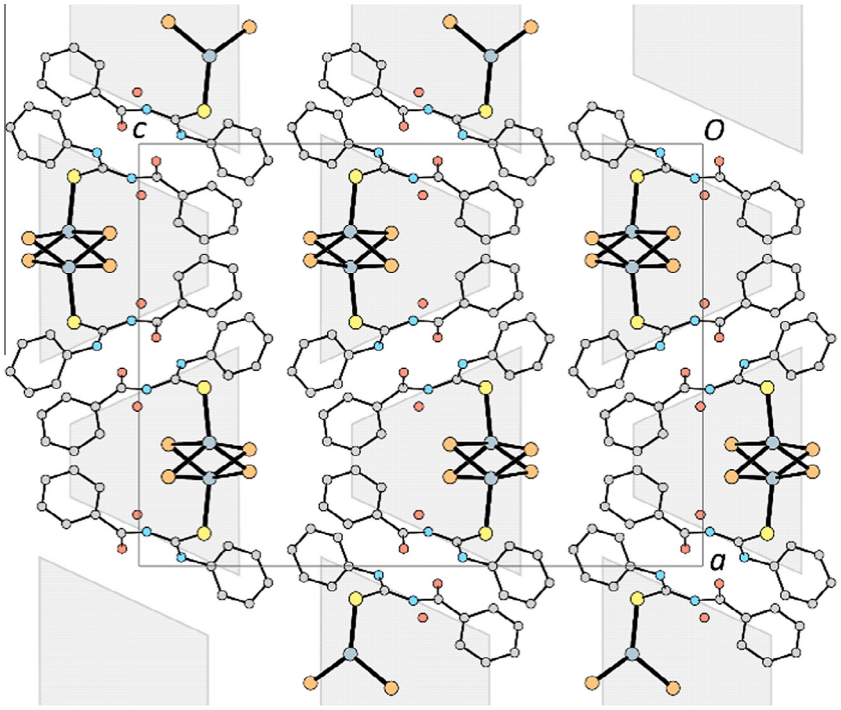

Fig. 8. Crystal packing in **2** seen along [0 1 0] direction. Hydrogen atoms are omitted for clarity.

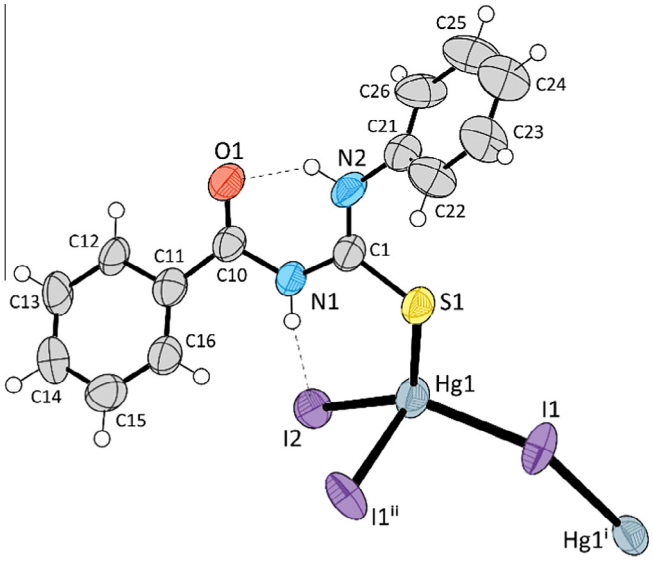

Fig. 9. Molecular structure of **3**. Ellipsoids are drawn at 50% probability level. Hydrogen bonds are denoted with dashed lines. Key bond lengths (Å) and angles (°) are: Hg1–S1 2.562(3), Hg1–I1 2.6743(12), Hg1–I2 2.6277(13), Hg1–I1^{ii} 3.3076(12), S1–Hg1–I1 98.58(8), S1–Hg1–I2 124.44(8), S1–Hg1–I1^{ii} 85.05(8), I1–Hg1–I2 135.95(4), I1–Hg1–I1^{ii} 94.10(3), I2–Hg1–I1^{ii} 98.21(3). Symmetry operations: (i) ½ − *x*, −½ + *y*, *z*; (ii) ½ − *x*, ½ + *y*, *z*.

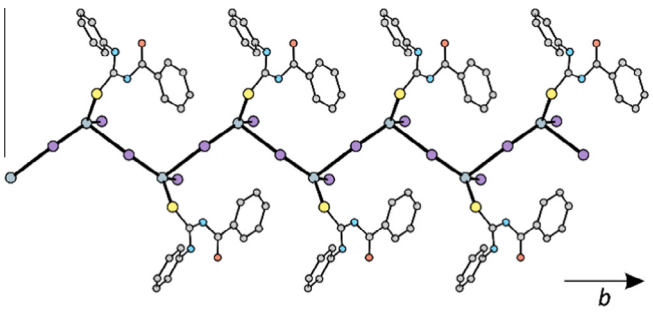

Fig. 10. Coordination polymer chain with $\not c11$ rod symmetry in structure of **3**. Hydrogen atoms are omitted for clarity.

3.5. Crystal structure of **5**

Compound **5** has similar coordination pattern to **3** and **4**. Mercury(II) is surrounded by three bromide anions and one bmtu molecule forming $HgBr_3S$ kernel with highly distorted tetrahedral geometry, $\tau_4 = 0.82$, $\tau'_4 = 0.81$ (Fig. 16). Br1 is a bridging ligand that allows the formation of coordination polymer with chain of $\not c11$ rod group symmetry spreading in [0 0 1] direction (Fig. 17). The identity period is similar to the ones observed in **2**–**4** regardless of different space group symmetry. Moreover, rods can be seen as trapezoidal prisms which align together to build 3D crystal structure.

Like before ligand adopts S-type conformation with **S**(6) hydrogen bond motif *via* N2–H···O1. Its bifurcation with N2–H···O1$^{[1-x,\ 1-y,\ 1-z]}$ leads to the formation centrosymmetric dimer similarly to **2** and **4** (Fig. 18). Hydrogen atom from the second N–H group is connected to bromide anion forming N1–H···Br1 hydrogen bond. All hydrogen bonds are summarized in Table 6 and visualized in Fig. 18.

In this structure there is a quite strong parallel-displaced $Cg1\cdots Cg1^{[-x,\ 1-y,\ 1-z]}$ stacking interaction with $d = 3.72$ Å, $\alpha = 0°$,

Table 4
Hydrogen bond parameters in structure of **3**.

	D–H (Å)	H···A (Å)	D···A (Å)	D–H···A (°)
N2–H2···O1	0.86	1.94	2.636(15)	137
N1–H1···I2	0.86	3.12	3.808(10)	139

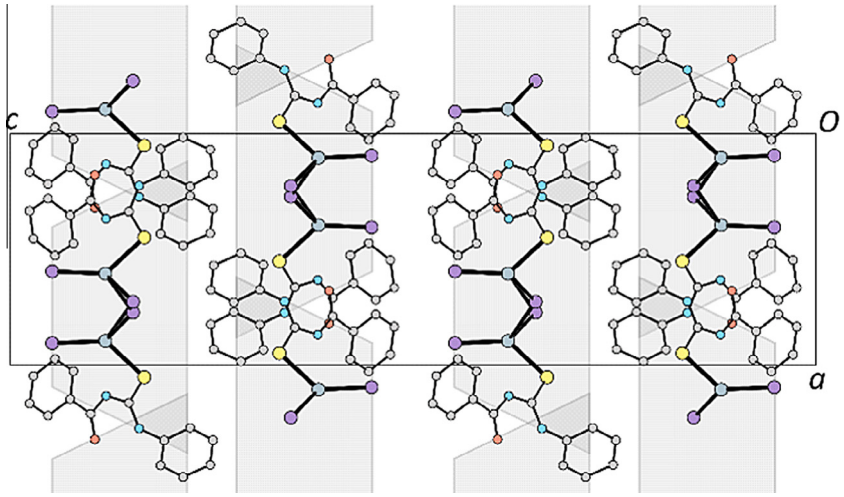

Fig. 11. Crystal packing in **3** seen along [010] direction. Hydrogen atoms are omitted for clarity.

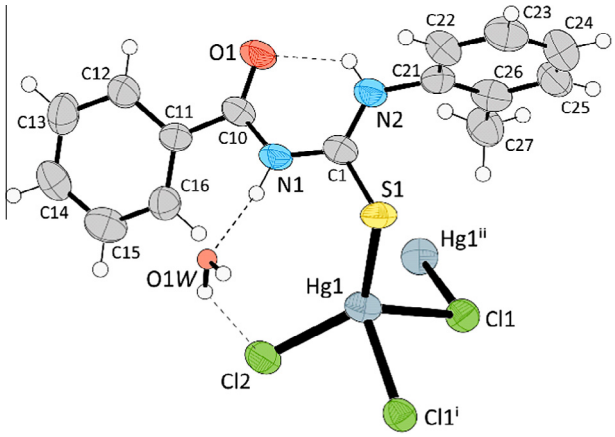

Fig. 12. Molecular structure of **4**. Ellipsoids are drawn at 50% probability level (except solvent molecule). Selected hydrogen bonds are denoted with dashed lines. Key bond lengths (Å) and angles (°) are: Hg1–S1 2.452(3), Hg1–Cl1 2.549(3), Hg1–Cl2 2.428(3), Hg1–Cl1^{i} 2.690(3), S1–Hg1–Cl1 110.10(9), S1–Hg1–Cl2 131.31(10), S1–Hg1–Cl1^{i} 104.35(8), Cl1–Hg1–Cl2 113.42(9), Cl1–Hg1–Cl1^{i} 92.64(8), Cl2–Hg1–Cl1^{i} 94.51(9). Symmetry operations: (i) ½ − *x*, −½ + *y*, *z*; (ii) ½ − *x*, ½ + *y*, *z*.

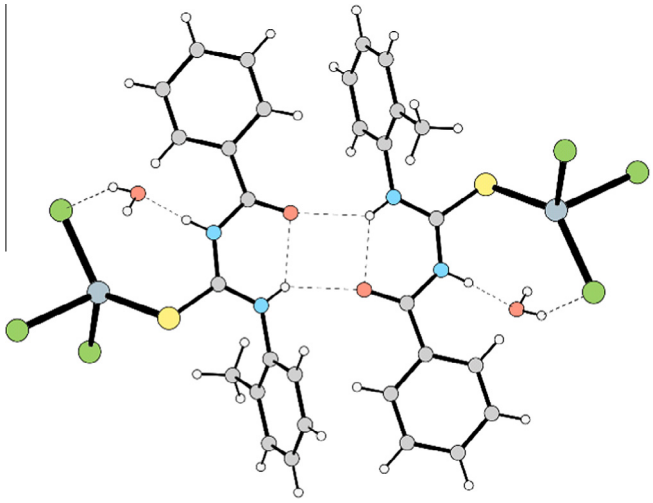

Fig. 14. Centrosymmetric dimer and hydrogen bond pattern found in structure of **4**. Hydrogen bonds are denoted with dashed lines.

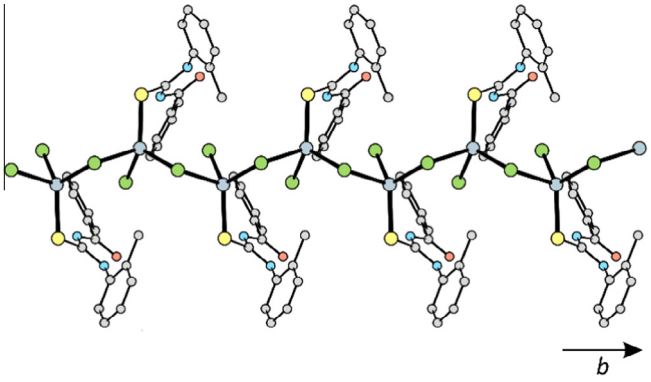

Fig. 13. Coordination polymer chain with $\not\parallel c11$ rod symmetry in structure of **4**. Hydrogen atoms and solvent molecules are omitted for clarity.

slippage = 1.47 Å. Dimers are additionally stabilized by T-shaped C12–H···*Cg*2$^{[1-x,\ 1-y,\ 1-z]}$ stacking interactions (d = 4.73 Å, α = 65°) that explains large twist of *o*-tolyl group in the relation to **S**(6) motif (see: Table s4). HOMA for *Cg*S1 ring is low in this case (0.67) and the ring does not participate in stacking interactions.

All described interactions make possible the formation of 3D structure (Fig. 19).

Table 5
Hydrogen bond parameters in structure of **4**. Symmetry operation: (a) −*x*, 2 − *y*, −*z*.

	D–H (Å)	H···A (Å)	D···A (Å)	D–H···A (°)
N2–H2···O1	0.86	2.01	2.676(12)	133
N2–H2···O1^{a}	0.86	2.38	3.107(11)	143
N1–H1···O1*W*	0.86	2.05	2.860(13)	157
O1*W*–H2*W*···Cl2	0.82	2.82	3.514(12)	145

3.6. Crystal structure of **6**

Compound **6**, like **1** has mononuclear structure with HgI_2S_2 kernel with highly distorted tetrahedral geometry (τ_4 = 0.82, τ'_4 = 0.73). Mercury(II) lies on twofold axis, so only one half of molecule is symmetrically independent (Fig. 20).

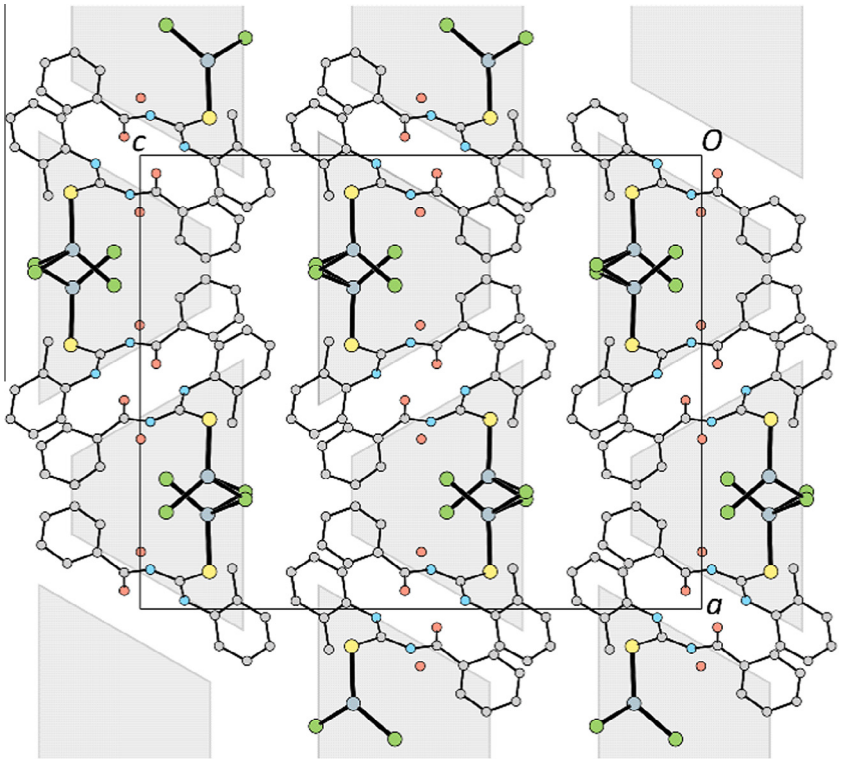

Fig. 15. Crystal packing in **4** seen along [0 1 0] direction. Hydrogen atoms are omitted for clarity.

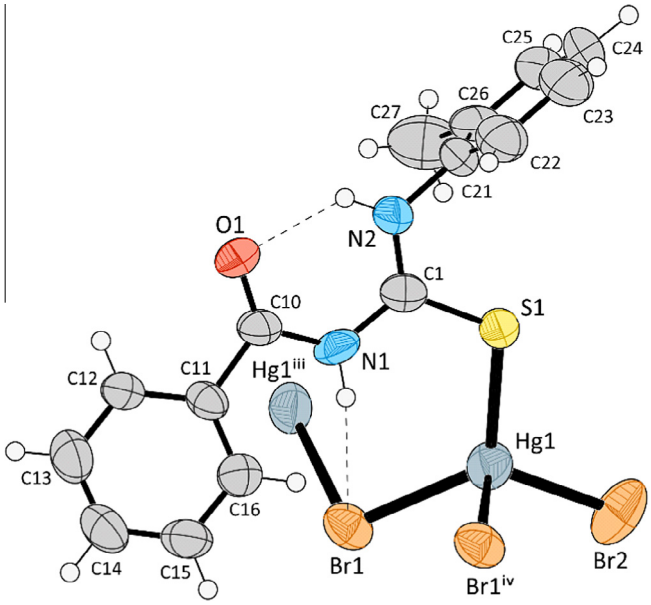

Fig. 16. Molecular structure of **5**. Ellipsoids are drawn at 50% probability level. Selected hydrogen bonds are denoted with dashed lines. Key bond lengths (Å) and angles (°) are: Hg1–S1 2.475(2), Hg1–Br1 2.5674(9), Hg1–Br2 2.4676(11), Hg1–Br1^{iv} 3.0519(11), S1–Hg1–Br1 119.79(6), S1–Hg1–Br2 113.26(6), S1–Hg1–Br1^{iv} 91.11(6), Br1–Hg1–Br2 124.16(4), Br1–Hg1–Br1^{iv} 88.74(3), Br2–Hg1–Br1^{iv} 106.93(5). Symmetry operations: (iii) $x, ½ - y, -½ + z$; (iv) $x, ½ - y, ½ + z$.

Ligand molecule adopts S-type conformation like in previously discussed structures, and **S**(6) motif is present due to N2–H···O1 intramolecular hydrogen bond. Second N–H group is incorporated in bifurcated N1–H···I1$^{[-x,\ y,\ ½-z]}$/N1–H···S1$^{[-x,\ y,\ ½-z]}$ hydrogen

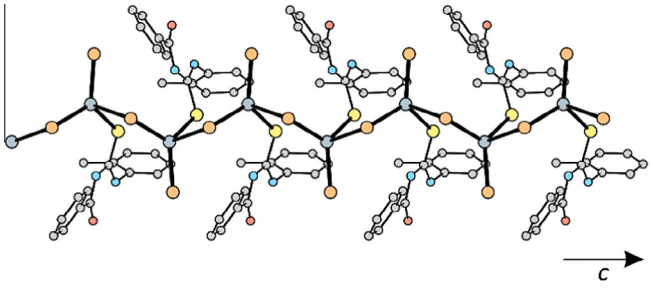

Fig. 17. Coordination polymer chain with $_{\infty}c11$ rod symmetry in structure of **5**. Hydrogen atoms are omitted for clarity.

bond. Hydrogen bonds are visualized in Fig. 20 and their parameters are given in Table 7.

The strongest parallel-displaced stacking interaction in this structure is $Cg2\cdots Cg2^{[½-x,\ -½-y,\ 1-z]}$, with $d = 3.94$ Å, $\alpha = 0°$, *slippage* = 1.62 Å. Like in **1**, the $Cg1\cdots CgS1^{[-x,\ -y,\ 1-z]}$ interaction can be found in this structure ($CgS1$ HOMA = 0.73), parameters are: $d = 3.72$ Å, $\alpha = 17°$. Large twist of *o*-tolyl group with respect to **S**(6) motif is probably caused by the formation of T-shaped C13–H···$Cg2^{[-½+x,\ -½+y,\ z]}$ stacking interaction ($d = 5.15$ Å, $\alpha = 90°$).

Packing diagram is presented in Fig. 21.

3.7. Comparative studies

The Cambridge Structural Database (CSD) v. 5.34 (Nov 2013 update) [38] contains structures of only two mercury complexes with 1-acylthiourea ligands: bis(1-benzoyl-3-(2-hydroxyethyl) bis(μ-chloro)dichlorothiourea-κ*S*)dimercury(II) [39] and bis(1-benzoyl-3-(2-chlorophenyl)thiourea-κ*S*)diiodomercury(II) (**6a**) [40]. Compound **6a** is not only similar to **6**, but also isostructural – both

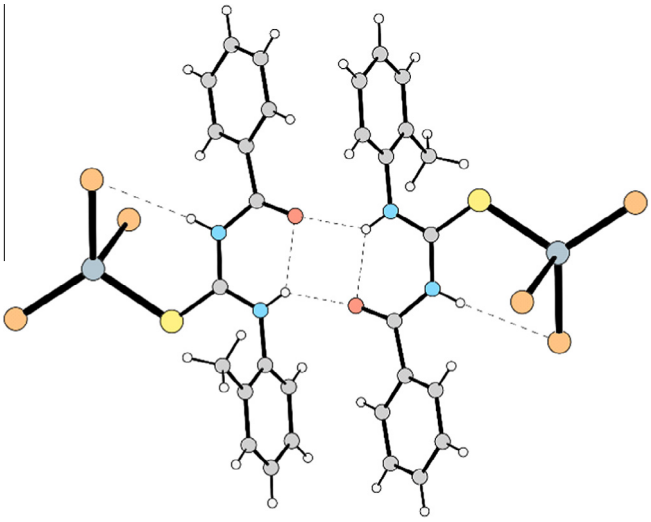

Fig. 18. Centrosymmetric dimer and hydrogen bond pattern found in structure of **5**. Hydrogen bonds are denoted with dashed lines.

crystalize in monoclinic space group *C*2/*c* with the twofold axis passing through mercury atoms. Unit cell identity parameter calculated for these structures is equal to $\Pi_{6,6a} = 0.005$ (for identical unit cells $\Pi = 0$). To quantitatively compare geometry of the molecules we have calculated isostructurality index and observed value is very high: $I'_{6,6a} = 0.97$ (for two identical structures $I' = 1$). Also the ligand molecule, 1-benzoyl-3-(2-chlorophenyl)thiourea [41] adopts very similar geometry to bmtu, however these compounds are not isostructural.

Table 6
Hydrogen bond parameters in structure of **5**. Symmetry operation: (a) $1 - x$, $1 - y$, $1 - z$.

	D–H (Å)	H···A (Å)	D···A (Å)	D–H···A (°)
N1–H1···Br1	0.86	2.83	3.603(7)	150
N2–H2···O1	0.86	2.03	2.680(9)	132
N2–H2···O1[a]	0.86	2.34	3.034(9)	137

The search of the CSD for compounds with Hg–S=C$(NR_2)_2$ moiety (where R = C or H) resulted in 54 structures with 3D coordinates determined. The most common are complexes with one mercury atom per complex molecule (42 cases). There are also 7 binuclear complexes and 1 structure of a trinuclear complex. Remaining 4 structures are *catena*-type 1D coordination polymers. Two of them (SAKBOV [42] and HGCLTU [43]) exhibit glide plane subperiodic symmetry (rod group $\not{}c11$, R5), and in two cases the polymeric chains go along twofold axes: BAPWEU [44] (rod group $\not{}112_1$, R9) and TURMCY [45] (rod group $\not{}222$, R13). Three first cases represent chains with alternating Hg and X atoms with one X atom and thiourea ligand additionally bounded to mercury atom terminally. Terminal Hg–X bonds are shorter than bridging Hg–X. Bond lengths Hg–S, usually close to 2.5 Å, in structure TURMCY are much longer (ca. 3.0 Å) as thiourea molecules are not terminal but bridging ligands. In 45 structures coordination number is equal to 4. Geometries of their kernels are usually highly distorted: $\tau_4 = 0.83(9)$, $\tau'_4 = 0.77(14)$. It can be easily seen that τ'_4 parameter better differentiates these structures (lower value and higher standard deviation). Remaining 9 structures contain mercury atoms with 2, 3, 5 and 6 coordination numbers.

As we have mentioned, compounds **2**–**5** form 1D polymeric chains. It is worthy to compare the identity periods for the rod

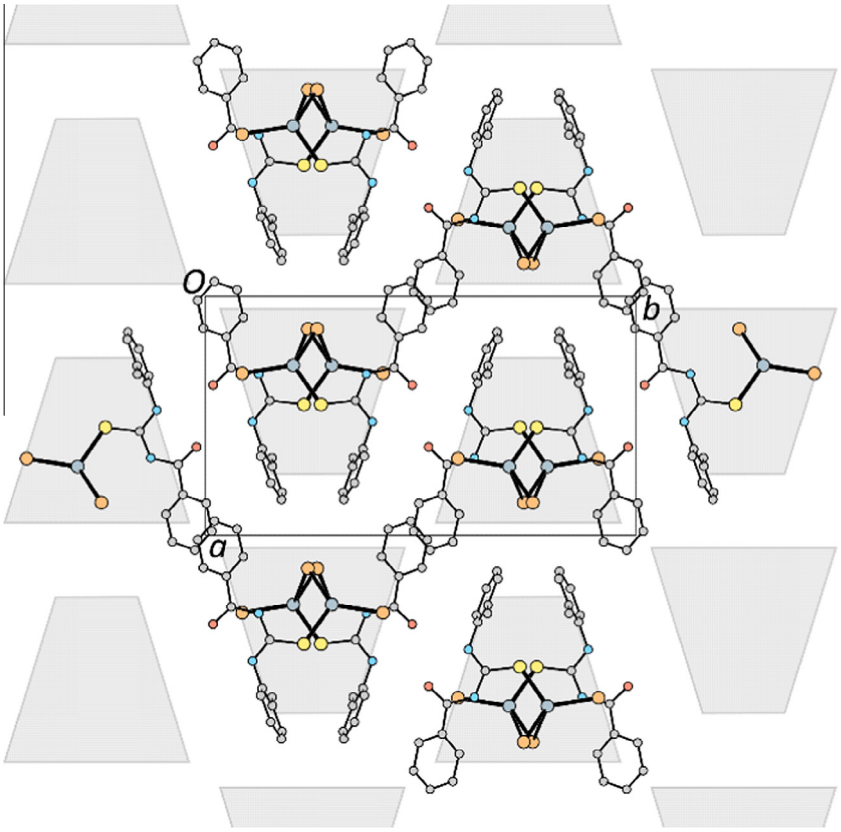

Fig. 19. Crystal packing in **5** seen along [001] direction. Hydrogen atoms are omitted for clarity.

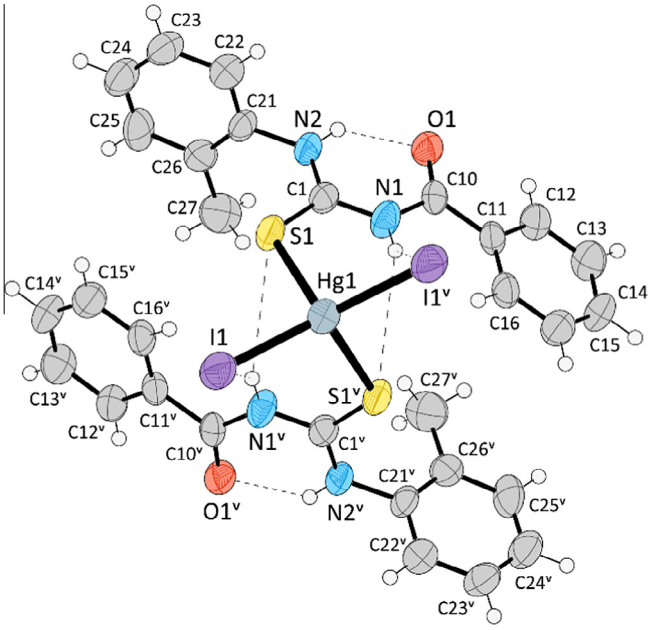

Fig. 20. Molecular structure of **6**. Ellipsoids are drawn at 50% probability level. Hydrogen bonds are denoted with dashed lines. Key bond lengths (Å) and angles (°) are: Hg1–S1 2.6774(18), Hg1–S1^{v} 2.6774(18), Hg1–I1 2.6672(9), Hg1–I1^{v} 2.6672(9), S1–Hg1–S1^{v} 100.37(8), S1–Hg1–I1 99.60(7), S1–Hg1–I1^{v} 108.13(6), S1^{v}–Hg1–I1 108.13(6), S1^{v}–Hg1–I1^{v} 99.60(7), I1–Hg1–I1^{v} 136.17(4). Symmetry operation: (v) $-x, y, ½ - z$.

Table 7
Hydrogen bond parameters in structure of **6**. Symmetry operation: (a) $-x, y, ½ - z$.

	D–H (Å)	H···A (Å)	D···A (Å)	D–H···A (°)
N1–H1···I1^{a}	0.86	3.37	4.024(6)	135
N1–H1···S1^{a}	0.86	3.15	3.882(7)	144
N2–H2···O1	0.86	1.95	2.612(9)	133

substructures. For $HgCl_2$ related: 7.5529(5) Å (**4**), $HgBr_2$ related: 7.5632(4) Å (**2**) and 7.8419(4) Å (**5**), as well as HgI_2 related: 8.7422(5) Å (**3**). Generally the period length increases with the size of halogen atom, but the influence of double bridging in **2** is clearly substantial and must be taken into account.

Table 8
M–X···H angles (°) found within N–H···X–M–L motif present in structures of title complexes (M = Hg) and in structures of compounds deposited in the CSD [38] (M = any).

	M = Hg L = bptu	M = Hg L = bmtu	Average	M = any L = any
X = Cl	72; 67	—	70	81(13)
X = Br	—	65	65	76(13)
X = I	60	60	60	71(16)

In complexes **1**–**6** the C=S bond length is clearly longer than in an isolated ligand molecule. The Hg–S distances depend on two factors: (1) the heavier the halogen, the longer Hg–S bond is, (2) bonds are longer for mononuclear complexes than for coordination polymers. Exactly the same trend can be observed for Hg–S=C angle. For detailed numerical data, see: Table s4.

Obviously Hg–X distances increase with halogen ion radius. Additionally it can be easily seen that in coordination polymers the Hg–X bridging bonds are unsymmetrical: some of them are shorter while others are longer by ca. 0.5 Å. This difference is the smallest in the case of **4** (only 0.14 Å). Numerical values for these distances are summarized in Table s4.

All angles at which electron-deficient hydrogen atoms are attracted to halogen atoms forming hydrogen bonds within discussed structures are acute (Table 8). Generally the Hg–X···H angle decreases as halogen atom mass increases, what is in a good agreement with values that can be found within structures deposited in the CSD. This effect is caused by anisotropic charge distribution in halogen atoms [46].

4. Conclusions

Mercury(II) halides readily form complexes with investigated thioureas. In compounds **2**–**5** one molecule of ligand is bounded to the metal atom and 1D polymeric chain is formed, while in compounds **1** and **6** the ratio Hg:L is 1:2 and the molecular crystals are obtained.

Common $_{p}c11$ rod group symmetry of polymer chains (**2**–**5**) allows simplified classification of the 3D packing as parallel stacking of trapezoidal prisms. The construction is reinforced by classic hydrogen bonds, parallel and perpendicular stacking interactions. The last ones can be correlated with conformation of aromatic rings and their deviation from planarity with respect to **S**(6) motif.

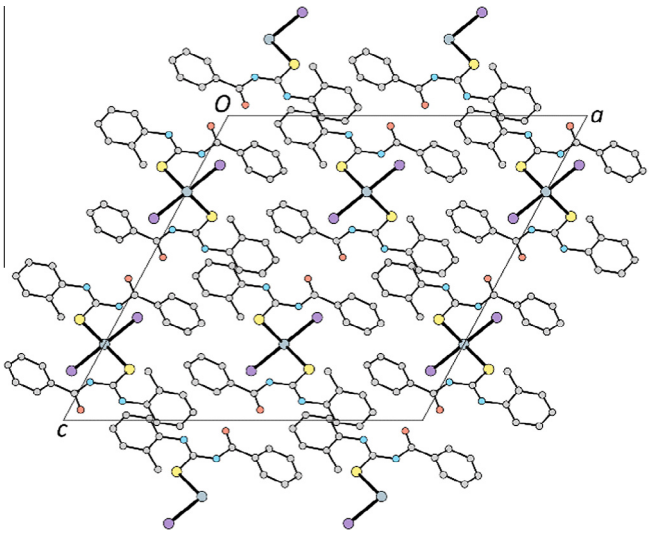

Fig. 21. Crystal packing in **6** seen along [010] direction. Hydrogen atoms are omitted for clarity.

In all structures ligand molecules adopt S-type conformation [35] with intramolecular N–H···O hydrogen bond forming **S**(6) motif [34]. We have analyzed geometries of 1-acylthiourea ligands among structures deposited in the CSD in one of our previous papers [47]. The second N–H group can serve as a donor for halogen atom (**1**, **3** and **5**), water molecule (**2** and **4**) or can be incorporated in bifurcated hydrogen bonds with S and I acceptors (**6**). This may explain the presence of additional water molecules in those structures.

Significant twist of aromatic rings in ligand molecules can be rationalized by the formation of non-parallel stacking interactions (T-shaped and edge-to-face).

Quite specific parallel-displaced stacking-type interactions involving pseudo-aromatic **S**(6) rings were found in five of the six discussed structures (HOMA $\geqslant$ 0.73). Weak aromatic character of **S**(6) motif in **5** (HOMA = 0.67) is probably the reason why such interactions are not present in this structure. In the CSD there are at least 153 structures where similar Ph···**S**(6) (Fig. 3) interactions (with $d < 4.4$ Å, $\alpha < 30°$) are present. The average value of HOMA in these structures is 0.78(5).

Acknowledgments

Financial support from the Polish Ministry of Science and Higher Education (project No. N N204 543339) is gratefully acknowledged.

Appendix A. Supplementary data

CCDC 971976–971981 contains supplementary crystallographic data for complex **1–6**. These data can be obtained free of charge via http://www.ccdc.cam.ac.uk/conts/retrieving.html, or from the Cambridge Crystallographic Data Centre, 12 Union Road, Cambridge CB2 1EZ, UK; fax: (+44) 1223-336-033; or e-mail: deposit@ccdc.cam.ac.uk. Supplementary data associated with this article can be found, in the online version, at http://dx.doi.org/10.1016/j.poly.2015.01.035.

References

[1] Ch.T. Elly, J. Water Pollut. Control Fed. 45 (1973) 940.
[2] A.R. Katritzky, O. Meth-Cohn, C.W. Rees, Comprehensive Organic Functional Group transformations, 1995, Pergamon Press, Elmsford, NY.
[3] W.J. Bruckard, G.J. Sparrow, J.T. Woodcock, Hydrometallurgy 33 (1993) 17.
[4] M.E. Mahmoud, M.M. Osman, M.E. Amer, Anal. Chim. Acta 415 (2000) 33.
[5] C.G. Moore, B. Saville, A.A. Watson, J. Appl. Polym. Sci. 3 (1960) 373.
[6] V. Ducháček, J. Appl. Polym. Sci. 22 (1978) 227.
[7] B. Mertschenk, F. Becka, W. Bauer, Ullmann's Encyclopedia of Industrial Chemistry: Thiourea and Thiourea Derivatives, 2011.
[8] A. Saeed, U. Flörke, M.F. Erben, J. Sulfur Chem. 35 (2014) 318.
[9] I.B. Douglass, F.B. Dains, J. Am. Chem. Soc. 56 (1934) 719.
[10] H. Stark, K. Purand, X. Ligneau, A. Rouleau, J.M. Arrang, M. Garbarg, J.C. Schwartz, W. Schunack, J. Med. Chem. 39 (1996) 1157.
[11] S. Cunha, F.C. Macedo Jr, G.A.N. Costa, M.T. Rodrigues Jr, R.B.V. Verde, L.C. de Souza Neta, I. Vencato, C. Lariucci, F.P. Sá, Monats. Chem. 138 (2007) 511.
[12] R.G. Pearson, J. Am. Chem. Soc. 85 (1963) 3533.
[13] J.G. Melnick, G. Parkin, Science 317 (2007) 225.
[14] V. Singh, V. Kumar, A.N. Gupta, M.G.B. Drew, N. Singh, New J. Chem. 38 (2014) 3737.
[15] A. Kumar, R. Chauhan, K.C. Molloy, G. Kociok-Köhn, L. Bahadur, N. Singh, Chem. Eur. J. 16 (2010) 4307.
[16] E. López-Torres, M.A. Mendiola, J. Organomet. Chem. 725 (2013) 28.
[17] A.A. Khandar, V.T. Yilmaz, F. Costantino, S. Gumus, S.A. Hosseini-Yazdi, G. Mahmoudi, Inorg. Chim. Acta 394 (2013) 36.
[18] E.J. Mensforth, M.R. Hill, S.R. Batten, Inorg. Chim. Acta 403 (2013) 9.
[19] H. Chiniforoshan, N. Pourrahim, L. Tabrizi, H. Tavakol, M.R. Sabzalian, B. Notash, Inorg. Chim. Acta 416 (2014) 85.
[20] G. Givaja, P. Amo-Ochoa, C.J. Gómez-García, F. Zamora, Chem. Soc. Rev. 41 (2012) 115.
[21] L.G. Donaruma, B.P. Block, K.L. Loening, N. Platé, T. Tsuruta, K.C. Buschbeck, W.H. Powell, J. Reedijk, Polym. Sci. USSR 28 (1986) 1240.
[22] B.M. Yamin, M.S.M. Yusof, Acta Crystallogr., Sect. E 59 (2003) o151.
[23] B. Zhang, B.-Q. Su, L. Xian, Acta Crystallogr., Sect. E 62 (2006) o4024.
[24] L.J. Farrugia, J. Appl. Crystallogr. 45 (2012) 849.
[25] G.M. Sheldrick, Acta Crystallogr., Sect. A 64 (2008) 112.
[26] A.W. Addison, T.N. Rao, J. Reedijk, J. van Rijn, G.C. Verschoor, J. Chem. Soc., Dalton Trans. (1984) 1349.
[27] L. Yang, D.R. Powell, R.P. Houser, Dalton Trans. (2007) 955.
[28] T.M. Krygowski, J. Chem. Inf. Model. 33 (1993) 70.
[29] H.R. Khavasi, M.A. Fard, Cryst. Growth Des. 2010 (1892) 10.
[30] H.R. Khavasi, A.R. Salimi, H. Eshtiagh-Hosseini, M.M. Amini, CrystEngComm 13 (2011) 3710.
[31] J.-Y. Wu, H.-Y. Hsu, Ch.-C.h. Chan, Y.-S.h. Wen, Ch. Tsai, K.-L. Lu, Cryst. Growth Des. 9 (2009) 258.
[32] L. Fábián, A. Kálmán, Acta Crystallogr., Sect. B 1099 (1999) 55.
[33] M. Kubicki, M. Szafrański, J. Mol. Struct. 446 (1998) 1.
[34] M.C. Etter, Acc. Chem. Res. 23 (1990) 120.
[35] M.G. Woldu, J. Dillen, Theor. Chem. Acc. 121 (2008) 71.
[36] H. Karabıyık, H. Karabıyık, N.O. İskeleli, Acta Crystallogr., Sect. B 68 (2012) 71.
[37] V. Kopský, D.B. Litvin, International Tables for Crystallography Volume E: Subperiodic Groups, 2010, International Union of Crystallography.
[38] F.H. Allen, Acta Crystallogr., Sect. B 58 (2002) 380.
[39] Y.-M. Zhang, L.-Z. Yang, Q. Lin, T.-B. Wei, J. Coord. Chem. 58 (2005) 1675.
[40] M.S.M. Yusof, B.M. Yamin, M.B. Kassim, Acta Crystallogr., Sect. E 60 (2004) m98.
[41] M.S.M. Yusof, B.M. Yamin, Acta Crystallogr., Sect. E 60 (2004) o1403.
[42] F. Cristiani, F.A. Devillanova, F. Isaia, G. Verani, L. Battaglia, A.B. Corradi, J. Chem. Res. 32 (1989) 301.
[43] P.D. Brotherton, A.H. White, J. Chem. Soc., Dalton Trans. 1 (1973) 2698.
[44] M. Cannas, F.A. Devillanova, G. Marongiu, G. Verani, J. Inorg. Nucl. Chem. 43 (1981) 2383.
[45] E. Moreno, L. Castro, An. R. Soc. Esp. Fis. Quim. A 67 (1971) 371.
[46] B. Bankiewicz, M. Palusiak, Struct. Chem 24 (2013) 1297.
[47] A. Okuniewski, J. Chojnacki, B. Becker, Acta Crystallogr., Sect. E 68 (2012) o619.